Applied Catalysis B: Environmental 163 (2015) 599–610

Contents lists available at ScienceDirect

Applied Catalysis B: Environmental

journal homepage: www.elsevier.com/locate/apcatb

Structure-reactivity relationship in catalytic hydrogenation of heterocyclic compounds over ruthenium black; Part B: Effect of carbon substitution by heteroatom

Katarzyna Morawa Eblagon [a,*], S.C. Edman Tsang [b]

[a] Faculty of Chemical Engineering, University of Porto, Rua Doutor Roberto Frias s/n, 4200-465 Porto, Portugal
[b] Wolfson Catalysis Centre, Department of Chemistry, University of Oxford, Oxford OX1 3QR, UK

ARTICLE INFO

Article history:
Received 13 May 2014
Received in revised form 20 August 2014
Accepted 22 August 2014
Available online 29 August 2014

Keywords:
Hydrogen storage
Liquid organic hydride
Heterocyclic compounds
Hydrogenation
Ruthenium catalysts

ABSTRACT

The effect of the type of heteroatom in the structure on the recyclability of possible candidate compounds for application as LOC (liquid organic carriers) was studied by comparing the rate and selectivity obtained in hydrogenation of carbazole, dibenzothiophene, dibenzofuran and fluorene. The effect of a partial saturation of the compound on its hydrogenation yield and reaction pathway was also considered by studying hydrogenation of 1,2,3,4-tetrahydrocarbazole. Using Ru black catalyst, the rate of hydrogenation was found to decrease in order; dibenzofuran > 1,2,3,4-tetrahydrocarbazole > carbazole » fluorene. No reaction was observed in the hydrogenation of dibenzothiophene under the conditions studied which was attributed to the immediate poisoning of ruthenium metal by sulphur compounds. The rate of hydrogenation of fluorene was around 3 times lower as compared to carbazole and over 8 times lower as compared to that of dibenzofuran under the same reaction conditions. With the exeption of S containing dibenzothiophene, the presence of the heteroatom in the structure was found to be beneficial in terms of increasing the rate of hydrogen loading step. Additionally, a higher reaction rate was obtained in the hydrogenation of the partially saturated 1,2,3,4-tetrahydrocarbazole as compared to the substrate carbazole. The structure and stability of intermediates was found to be significantly influenced by the type and presence of a heteroatom in the structure. A stable octahydro-intermediate was observed only with N-heterocycles, whereas a stable hexahydro-intermediate was produced in the polyaromatic hydrocarbon-fluorene. Additionally, the theoretically obtained lowest total enthalpies using DFT calculations agreed well with the stable intermediates observed experimentally in the hydrogenation of fluorene. Theoretical DFT differences in enthalpies also indicated the products of hydrogenolysis of perhydro-dibenzofuran to be the most favourable products of its hydrogenation, which agreed well with the experimental observations. Overall, taking into account the recyclability of LOC, substitution of carbon with a N heteroatom was demonstrated to be one of the promising approaches to improve the kinetics of the hydrogen loading step.

1. Introduction

Hydrogen is considered a vector of a clean and sustainable future energy, addressing the need for independence and security around the globe. With this regard, it represents a promising alternative to the ever-increasing use of fossil fuels [1,2]. With the so-called "Hydrogen Economy" put in place, there is a constant need for development of a feasible, cost-effective and safe hydrogen storage and distribution media [3,4]. Commodity chemicals, potential liquid organic carriers (LOC) such as cyclohexane [5], methylcyclohexane [6–8], decalin [9], carbazole and 9-ethylcarbazole [10–12] or boron–nitrogen heterocycles like borazine [13] have been long investigated for application as hydrogen storage media [14,15].

The influence of the structural features of the LOC material on the dehydrogenation step has been extensively studied [13,16–18]. For example, it has been found that the substitution of C by a heteroatom, mainly N or O, in the LOC ring structure drastically decreases the temperature of dehydrogenation of the corresponding aromatic compound by diminishing the strength of neighbouring α-CH bonds in the ring [17]. The introduction of a heteroatom was further reported to diminish the absolute value of the standard enthalpy of hydrogenation, thus resulting

* Corresponding author.
E-mail address: keblagon@fe.up.pt (K.M. Eblagon).

http://dx.doi.org/10.1016/j.apcatb.2014.08.040
0926-3373/

in lower barriers for dehydrogenation [19]. In addition, a significant electronic effect caused by electron donating substituents on the ring was identified to substantially increase the rate of dehydrogenation [16]. Additionally, the dehydrogenation reaction of the LOC candidate materials studied in the present work has also been reported. For example, perhydro-carbazole (fully loaded carbazole) was dehydrogenated over 5% Rh/C catalyst at 125 °C and 1 bar hydrogen. Under these relatively mild conditions, a high conversion of 84% was obtained with 50% selectivity to tetrahydrocarbazole (removed 8 hydrogen atoms from perhydro-carbazole) and 12% to carbazole (fully dehydrogenated carrier) among other products [19]. Furthermore, a slow rate of perhydro-dibenzofuran dehydrogenation was reported by Wang [20] using homogenous iridium pincer complexes. In this work, a complete conversion of the substrate was achieved in the presence of a hydrogen acceptor (tert-butylethylene) at 200 °C during 24 h but with poor selectivity of 60% to octahydro-dibenzofuran. Substituted thiophenes were also proposed for hydrogen storage materials [21]. Sotoodeh [22] attempted dehydrogenation of cyclic carbohydrate perhydrofluorene (6.74% of theoretical hydrogen uptake) over a 5 wt% Pd on activated carbon catalyst at 170 °C under continuous flow of He.

On the other hand, there is only scarce amount of works dealing with the impact of the chemical structure of the LOC material on the hydrogenation step [17,23–25]. The often neglected fuel regeneration step (hydrogen loading) is assumed to be taking place off-board of the vehicle where much harsher conditions can be used than those required for an on-board dehydrogenation step. In spite of that, the LOC recyclability should be considered in the search for an appropriate H_2 carrier material as it is unquestionably an important parameter from both economic and environmental points of view. Thus, it is important to study the parameters of the off-board hydrogen loading step to optimise cost and to avoid production of waste which would render a more competitive and feasible H_2 storage strategy. Correspondingly, in our previous works, we have focused on the influence of the catalytic system on the hydrogenation of 9-ethylcarbazole as a prototype of LOC [10,26,27]. We have found that the hydrogenation of this compound over a ruthenium black catalyst results in the production of a very stable intermediate (9-ethylcarbazole, which corresponds to the addition of 8 hydrogen atoms to the substrate, abbreviated +8 [H]). Interestingly, we observed that further hydrogenation of this compound was strongly hindered by its geometry affecting its adsorption on the catalyst surface [10]. Following these findings, it was decided to focus on the influence of the chemical structure of the LOC material on its reactivity in the hydrogenation reaction. In this regard, in Part A of the present work [28] we investigated the influence of the number of fused aromatic rings (acridine vrs carbazole) and the presence and length of a side chain (9-ethylcarbazole ethanol, 9-ethylcarbazole and carbazole) on the rate and selectivity of hydrogenation over a commercial Ru black catalyst. On the other hand, the present study is a continuation of the previous investigations that focuses on the influence of the presence and type of heteroatom in the structure as well as partial hydrogenation of LOCs on their reactivity during the hydrogen loading step using the same Ru black catalyst. Finally, a set of guidelines leading to the design of a more effective and eco-friendly hydrogen storage materials for LOC based hydrogen storage methodology will be discussed.

2. Experimental

2.1. Materials

1,2,3,4-Tetrahydrocarbazole (99% purity), Carbazole (≥95%), Fluorene (98%), Dibenzofuran (98%), Dibenzothiophene (≥98%), 1,4-Dioxane (99%) and Ru black commercial catalyst were purchased from Sigma Aldrich and used as received. Hydrogen gas (99.9%) was supplied by Air-Products.

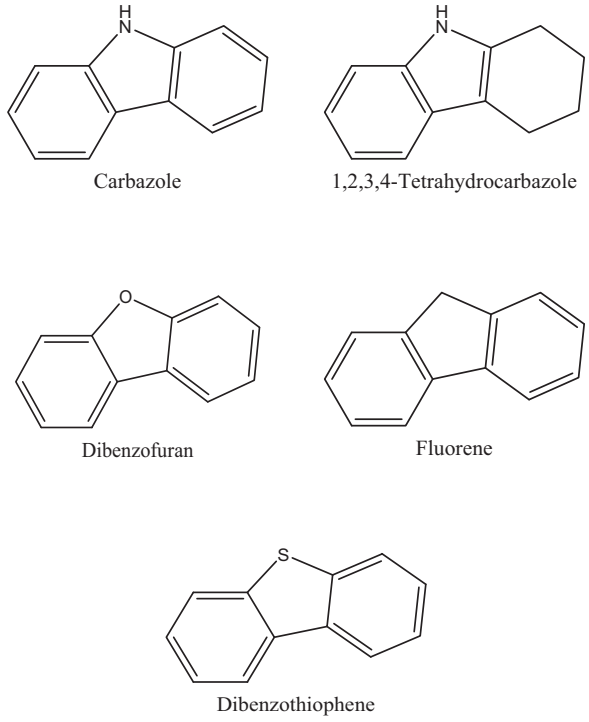

Fig. 1. Organic molecules studied in the present work for application in LOC based hydrogen storage methodology.

The structures of the LOC compounds are depicted in Fig. 1. The investigated structural factors included: type of heteroatom substituting carbon in five-membered ring and the effect of partial saturation of one of the benzenoid rings in the carbazole substrate (hydrogenation of 1,2,3,4-Tetrahydrocarbazole).

The choice of the Ru black catalyst was motivated by the geometry of its active sites, which resulted in the production of a very stable intermediate (Pl 8 [H]–addition of 8 hydrogen atoms to the 9-ethylcarbazole substrate) in the hydrogenation of 9-ethylcarbazole [10]. The aim of the present work is to gain an insight into which structural features of the LOC candidate compounds directly influence the production of stable intermediates during hydrogenation over the same Ru black commercial catalyst.

2.2. Hydrogenation reactions

The hydrogenation reactions of the heterocyclic compounds shown in Fig. 1 were performed in a set of conditions optimised previously for the hydrogenation of 9-ethylcarbazole [10]. In a typical experiment, 3 grams of substrate (Fig. 1) was dissolved in 100 ml of 1,4-dioxane solvent with the aid of an ultrasonic bath where needed, followed by the addition of 0.15 g of Ru black catalyst. Subsequently, the mixture was sealed in a Parr stainless steel reactor equipped with a thermocouple and a pressure gauge. The reaction mixture was magnetically stirred and heated to 130 °C at 1 bar of H_2. When the desired temperature was reached, 70 bar of hydrogen was charged into the reactor and the reaction time was measured. In order to obtain the change of concentration of the intermediates and products in time, aliquots of reaction mixture were withdrawn from the reactor periodically for analysis of their composition by Gas Chromatograph-Mass Spectrometer (GC-MS) as described in our previous work [10]. Control experiments were carried out, in which the hydrogenation reaction of 9-ethylcarbazole over the Ru black catalyst was tested four times under same reaction

conditions and the results showed a variation within 5% in the values of conversion and selectivity. In addition, the carbon balance was estimated for all of the reactions in the acceptable range of 87–95%.

2.3. Product analysis and reaction modeling

The structures of the final products and intermediates of the reactions were assigned based on their mass spectra and the database available with the GC-MS system used. Before analysis, individual calibration curves were prepared for each of the reactions analyzed by running at least five different concentrations of substrate. The time–temperature program for the GC-MS analysis was varied according to the structure of the molecules of interest. The standards of most of the intermediates and products were not available commercially, therefore their response factor was assumed to be 1 for the calculation of the concentrations.

The conversion of the starting material was calculated based on the amount of substrate found in the reaction mixture during each on-line sampling as compared to the quantity present at the beginning of the reaction. The selectivity was calculated using Eq.2.3.1., shown below;

$$\text{Selectivity}\,(\%) = \frac{\text{amount of selected product (moles)}}{\text{sum of all products (moles)}} \times 100\% \quad (2.3.1)$$

Based on the concentration versus time profiles, the reaction models were developed and subsequently the rate constants of the intermediate reactions were calculated according to a method described in detail in our previous works [10,27,28]. All the calculations were performed using Matlab (version 7.5).

2.4. DFT theoretical calculations of total enthalpy

The theoretical stability of the products and intermediates of hydrogenation of fluorene and dibenzofuran were computed using DFT calculations of the total enthalpy and compared with the experimental observations. These calculations gave valuable information on the influence of the type of heteroatom or absence of heteroatom on the structure of the stable intermediates and products formed during hydrogenation of the substrates. The DFT calculations of the total enthalpy for each individual product and intermediate were performed using Gaussian 03 software [29] and were described elsewhere in detail [10,28]. All the calculations were performed with 6-311+G(3df, 2p) basis set, which provided the electronic energy for the geometry optimised molecules and a B3LYP hybrid functional for electron correlation method [30]. The same basis set was used for the estimation of the vibrational frequencies. The thermodynamic parameters of products and intermediates involving transitional, rotational and translational modes were all taken into consideration. Subsequently, the calculated total enthalpy (the sum of electronic energies found from geometry calculations, and thermal, translational and vibrational energies) was compared to the sum of enthalpies for the starting material together with the total enthalpy of the moles of hydrogen added to create the defined intermediate, according to the formula given in Eq.2.4.1 where H is the sum of enthalpies and n is the number of moles of hydrogen added to the starting material.

$$H_{\text{starting material}} + n \cdot H_{H_2} = H_{\text{intermediate product}} \quad (2.4.1)$$

All of the calculations were done in gas phase approximation at 403 K. It is noted that due to the gas phase approximation the results of these DFT calculations can serve only as guidelines for stability trends of various intermediates produced during these reactions as explained in detail in part A of the present work [28].

3. Results

3.1. Catalyst characterization

The ruthenium black catalyst was characterized in our previous work [10,28]. In short, the CO pulse chemisorption on Ru black catalyst showed dispersion of 1% and a metal surface area of 4.8 m^2/g with a BET surface area of 22 m^2/g. The HRTEM study of the dispersion of the catalyst particle size of Ru black showed that the particles are highly aggregated with an approximate mean diameter of 6 nm. The CO-IR study showed that the main active sites of the catalyst have a flat geometry [10]. The XPS study revealed two ruthenium species present on the surface, namely ruthenium metallic and oxidized ruthenium (RuO_2) as well as some carbonaceous species originating from the synthesis method of the catalyst. The Ru black catalyst was used without any in-situ activation.

3.2. Influence of the partial saturation of the fused rings on hydrogenation reactivity. Comparison of hydrogenation of carbazole (CAR) and 1,2,3,4-tetrahydrocarbazole (THC)

The influence of a partial hydrogenation of one of the fused rings on the LOCs reactivity in the hydrogenation reaction was studied. Additionally, the absence of carbazole aromatic substrate in the reaction mixture on the hydrogenation pathway of 1,2,3,4-tetrahydrocarbazole was considered. The hydrogenation of CAR was described in detail in Part A of the present manuscript [28]. In short, an analysis of the products from the hydrogenation of carbazole showed the following: tetrahydro-carbazole (Pl 4 [H]), hexahydro-carbazole (Pl 6 [H]), octahydro-carbazole (Pl 8 [H]) and three stereoisomers of the fully hydrogenated perhydro-carbazole (Pl 12 [H] A, B, C). Three possible reaction pathways were observed in the hydrogenation of carbazole over the studied ruthenium black catalyst. The first one was a consecutive hydrogenation of carbazole via flat adsorption on the surface of the catalyst, via formation of 1,2,3,4-tetrahydrocarbazole (THC), and Pl 8 [H] intermediates, resulting in the formation of a cis-isomer of perhydro-carbazole Pl 12 [H] B which was the predominant fully saturated product. Another parallel route was the stepwise formation of the Pl 12 [H] A trans-isomer via the Pl 6 [H] isomer. The last possible hydrogenation pathway of carbazole was the direct formation of a trans-isomer of the fully loaded perhydro-carbazole Pl 12 [H] C. Thus, it should be noted that the dearomatization of 1,2,3,4-tetrahydrocarbazole is inevitably an intermediate step in the sequential hydrogenation of CAR.

In order to elute the influence of the partial saturation of the side benzenoid ring fused to the N-heterocyclic ring, the hydrogenation of 1,2,3,4-tetrahydrocarbazole substrate was carried out under the standard reaction conditions used for CAR hydrogenation in the first part of the present work [28]. It should be noted that with the addition of a hydrogen atom to at least one of the carbon-carbon double bonds and the destruction of the aromaticity of the system the molecule is known to be activated for hydrogenation. The hydrogenation of carbazole which is a non-basic compound into 1,2,3,4-tetrahydrocarbazole, makes the lone electron pair more localized on the nitrogen heteroatom rather than donated to the Π-conjugated system. Thus, 1,2,3,4-tetrahydrocarbazole (THC) displays a more basic character than CAR. Therefore in theory it should be more facile to hydrogenate than CAR due to the improved adsorption capacity of THC on the catalyst surface since basic compounds were previously reported to display higher hydrogenation rates than their non-basic counterparts [31,32]. The change of the concentration experimentally obtained for the products and intermediates in time during the hydrogenation reaction of THC over ruthenium black catalyst are shown in Fig. 2. The products of the hydrogenation of THC are marked starting from the addition of four

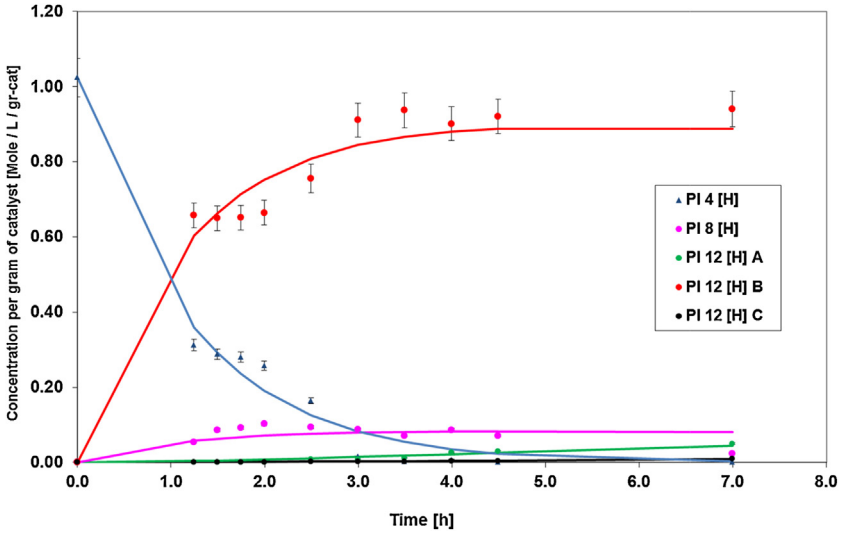

Fig. 2. Concentration versus time for substrate, products and intermediates in the hydrogenation of THC over a ruthenium black catalyst. Pl 4 [H] is 1,2,3,4 tetrahydro-carbazole (substrate), Pl 8 [H] is octahydro-carbazole, Pl 12 [H] A,B,C are the fully saturated isomers of perhydro-carbazole.

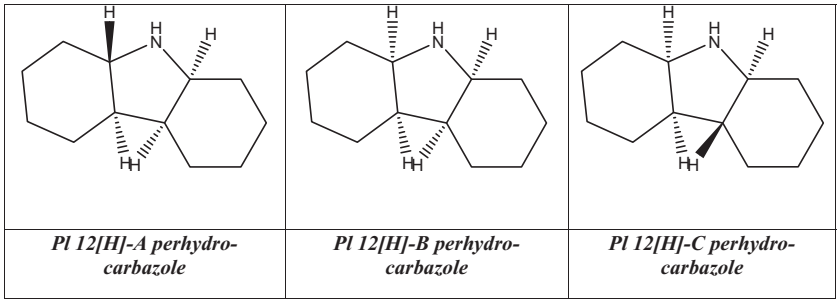

Fig. 3. Three stereoisomers of the fully hydrogenated carbazole [28].

hydrogen atoms (Pl 4 [H]-1,2,3,4-tetrahydrocarbazole substrate) to facilitate comparison with the rate constants obtained for the hydrogenation of CAR reported in the first part of the present work [28]. It should be noted that in the hydrogenation of CAR, THC is one of the main intermediates.

The products identified by means of GC-MS analysis in hydrogenation of THC were: octahydro-carbazole (Pl 8[H]) and three isomers of the fully saturated perhydro-carbazoles (Pl 12 [H] A, B, C). The structures of these isomers are shown in Fig. 3 [28].

It is interesting to note that on the contrary to the previously described hydrogenation of CAR, not even a trace of hexahydro-carbazole (Pl 6 [H]) was detected in the hydrogenation of THC. This result can suggest that the production of the Pl 6 [H] intermediate takes place directly from the starting material (CAR) and it is not a result of a subsequent addition of two hydrogen atoms to THC (Pl 4 [H]) intermediate. This result supports our model developed for CAR hydrogenation presented in Part A of the present work [28].

The proposed model for THC hydrogenation over ruthenium black catalyst is shown in Fig. 4 in comparison to the hydrogenation of THC as an intermediate product during the hydrogenation of CAR.

As it can be seen from this figure, in the presence of CAR, there is a direct conversion of Pl 8 [H] to Pl 12 [H] A trans-isomer. This reaction does not take place when the substrate is THC. Therefore, it can be suspected that when the reaction is starting from CAR as a substrate, two stereoisomers of Pl 8 [H] are obtained; cis and trans as shown in Fig. 5.

In spite of the fact that the two isomers of Pl 8 [H] were not observed by means of GC-MS in the present work, it is possible that they were not separated on the column due to the similar physical properties of these molecules. However, based on the developed model, when CAR is used as a substrate, the trans-Pl 8 [H] can be converted to trans-isomer of perhydro-carbazole Pl 12 [H] A. On the other hand, when THC is used as a starting material, the addition of

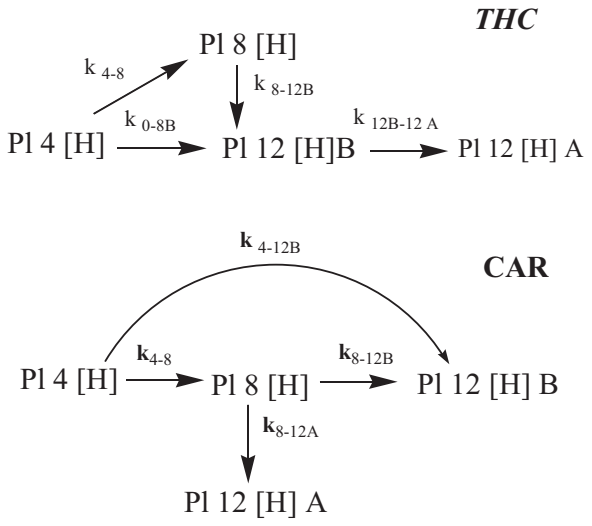

Fig. 4. Comparison of the developed models for hydrogenation of 1,2,3,4 tetrahydrocarbazole (Pl 4 [H]) as a substrate (top diagram) with the modeled hydrogenation pathway of the same compound (Pl 4 [H]) but as an intermediate in hydrogenation of carbazole (part of the hydrogenation of CAR as a substrate) in the bottom.

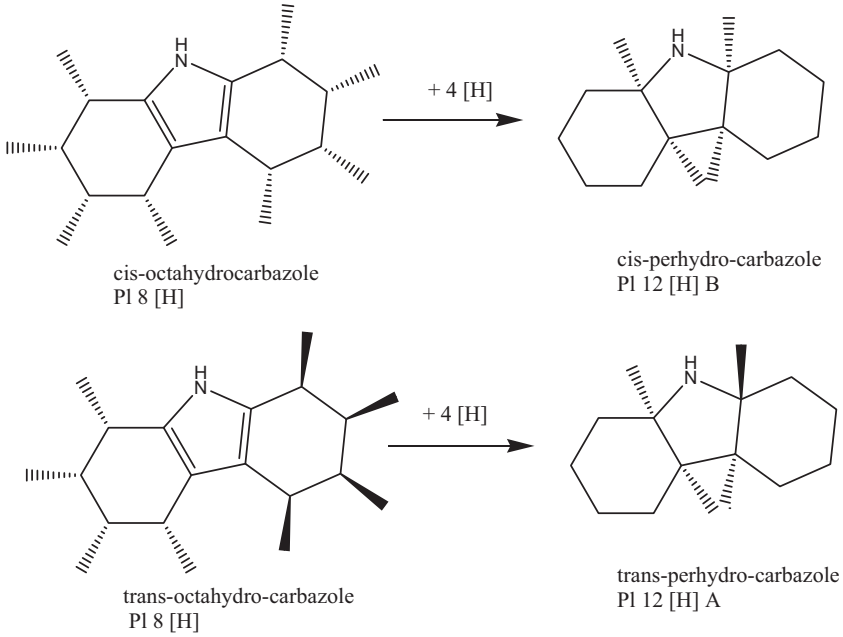

Fig. 5. Hydrogenation of cis- and trans-isomers of octahydro-carbazole into fully saturated perhydro-carbazoles.

the 4 hydrogen atoms is taking place solely on the same side of the molecule leading to the production of cis Pl 8 [H] and subsequently the cis-stereoisomer of perhydro-carbazole Pl 12 [H] B. In addition, the presence of CAR in the reaction mixture inhibits the isomerisation of Pl 12 [H] B to Pl 12 [H] A, as it can be seen in Fig. 4. It becomes thus clear that the hydrogenation pathway can be altered by the selective occupation of active sites by the substrate. Due to the fact that the electronegative densities on the aromatic rings and on the nitrogen atom have identical levels in CAR [33], it adsorbs preferentially with the molecular plane parallel to the surface, thus occupying an assembly of active sites on the surface of the catalyst. Flat adsorption mode not only allows CAR to maximize the delocalized absorbate–substrate covalent interaction but also increases the Van der Walls interaction with the surface of the catalyst [24]. On the contrary, the geometry of the fully saturated Pl 12 [H] allows these molecules to adsorb exclusively in the orientation perpendicular to the catalyst surface. However, taking into consideration that CAR is occupying most of the planar sites on the catalyst and the scarcity of the unsaturated sites on Ru black catalyst, the side-on geometry of adsorption is not favourable. On the other hand, in the absence of adsorbed CAR on the catalyst surface, the side-on adsorption takes place due to higher abundance of active sites on ruthenium black leading to the isomerisation of Pl 12 [H] B to Pl 12 [H] A. It is noteworthy that most of the hydrogenation steps are the same in the case of THC as a substrate and intermediate of the reaction. Nevertheless, the presence of a strongly adsorbing aromatic substrate such as CAR alters the overall path of the reaction, inhibiting the isomerisation of the saturated compounds from taking place. It is noteworthy that in the hydrogen storage application, the isomerisation following the hydrogenation step of the fully loaded LOC should be avoided, due to the more rigid geometric structure of the fully loaded trans-isomers as compared to cis-isomers and associated foreseen problems with adsorption of the trans-isomers on the catalyst surface during dehydrogenation [24,34]. It should be noted that the developed model for hydrogenation of THC agrees well with the experimental results as depicted in Fig. 2. In order to display more clearly the relevance of the proposed kinetic model, an enlarged part of Fig. 2 containing the products and intermediates which appeared at low concentration is included in Supplementary material, Figure 1s.

In order to elute the influence of the absence of the aromatic ring from CAR on the rate of hydrogenation of Pl 4 [H], the calculated rate constants of the hydrogenation of THC as a substrate and intermediate in the presence of CAR were compared. The results of the calculated rate constants of the intermediate reactions for THC and CAR hydrogenation are gathered in Table 1.

Comparison of the k_0 values shows that the rate of hydrogenation of THC is around 30% higher than the rate of hydrogenation of CAR. The conversion of THC to the Pl 8[H] intermediate is almost three times higher in the absence of CAR. This finding can be explained by two factors, the lack of aromatic stability of the benzenoid rings in the case of THC, which renders the molecule more susceptible to hydrogenation and the absence of CAR adsorbed flatly on the catalyst surface. THC which on the other hand contains only one aliphatic ring was reported to absorb at an angle of 30° away from the metal atom, in a less stable adsorption mode [35] leading to higher rates of hydrogenation. Similar results were also reported in the study of naphthalene hydrogenation to decalins via tetralin [24]. Additionally, there is a significant difference between the rate constant for the conversion of Pl 8 [H] into Pl 12 [H] B for CAR and THC. Interestingly, the rate constant for THC is 100 times higher in the absence of CAR. This is evidence that CAR adsorbs strongly on the catalyst surface, which was previously observed in the dehydrogenation of perhydro-carbazole over a Pd catalyst [18]. It seems that there could be a competition for active sites between CAR and THC.

Higher selectivity values towards the fully hydrogenated compounds were recorded for 1,2,3,4-tetrahydrocarbazole. The partially saturated molecule also showed a lower selectivity towards formation of the intermediate with the intact middle

Table 1
Comparison of the first order rate constants obtained for intermediate reactions in hydrogenation of 1,2,3,4-tetrahydrocarbazole (THC) and carbazole (CAR).

Rate constant (h^{-1})	THC	CAR
k_0	0.84	0.57
$k_{4\text{-}8}$	0.84	0.3
$k_{4\text{-}12B}$	0.3	0.89
$k_{8\text{-}12B}$	3.0	0.03

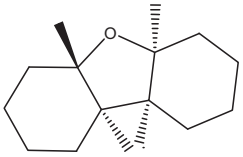

Pl 12 [A]-trans perhydro-dibenzofuran

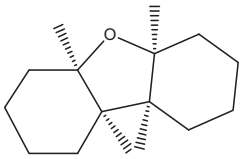

Pl 12 [B]-cis perhydro-dibenzofuran

Fig. 6. Cis- and trans stereoisomers of perhydro-dibenzofuran.

"pyrrole" ring (Pl 8 [H]) as compared to CAR. The rate constant of Pl 8[H] formation in THC is lower than the rate of its disappearance whereas in the case of CAR the relation is reversed and the subsequent conversion of Pl 8 [H] to the fully saturated product is very sluggish. It should be noted that no side reactions such as ring opening or C—C bond rupture were observed in the hydrogenation of neither CAR nor THC, under the reaction conditions studied.

3.3. Influence of the type of heteroatom in the five-membered heterocyclic ring

In general, the introduction of a heteroatom, besides changing the C—C bond lengths and distorting the ring geometry can result in a reduction of the π-electron density in the aromatic ring when the introduced heteroatom is more electronegative than carbon (N and O). In addition, the introduction of a heteroatom to the structure of polycyclic aromatic compound results in a change in the strength of the interaction of the heterocyclic ring with the surface of the catalyst than the remaining fused rings in its structure [34]. As a consequence of the charge redistribution, the geometry of adsorption of this type of molecules is tilted from the flat surface of the catalyst. Additionally, one of the factors influencing the hydrogenation activity of the molecule is its aromaticity. The aromaticity of the heterocycles decreases in order of substituted heteroatoms as follows S > N > O [36]. Thus, the highest aromaticity of thiophene analogues can be explained by almost equal electronegativity of sulphur as compared to carbon as well as its covalent radius only slightly higher than that of carbon. As a result, there is only a slight distortion in geometry of the fused rings containing the S heteroatom in the structure.

3.3.1. Hydrogenation of dibenzofuran (O)

Dibenzofuran is a heteroaromatic compound (aromatic ether) which can be classified as basic due to the fact that it contains a lone pair of electrons residing in a p orbital of oxygen that is not involved in the formation of the aromatic electron cloud. In addition, the other pair of electrons in the oxygen atom that is not involved in the covalent bonding with neighboring C atoms forms a delocalized Π-orbital [37].

In the hydrogenation of commercially available dibenzofuran over ruthenium black catalyst in the present work, the following products were identified; tetrahydro-dibenzofuran (Pl 4 [H]), octahydro-dibenzofuran (Pl 8 [H]), and two isomers of the fully saturated perhydro-dibenzofuran (Pl 12 [H] A, B shown in Fig. 6).

In addition to these products, three other by-products were identified, which originated from the ring opening reaction (hydrogenolysis) of the fully hydrogenated perhydro-dibenzofurans. These products were: bicyclohexyl (BCH), bicyclohexyl-2-one (BCHO) and cyclohexylcyclohexanol (CHCH). The structures of the products of ring opening of perhydro-dibenzofuran are shown in Fig. 7. The absence of biphenyl and its analogues suggests that the ring opening reaction and oxygen removal took place after the hydrogenation of dibenzofuran was completed. Generally, if the oxygen is inserted into an aromatic ring, the hydrogenation of this ring is considered to be an essential step prior to the C–O scission [37]. The hydrogenation of two

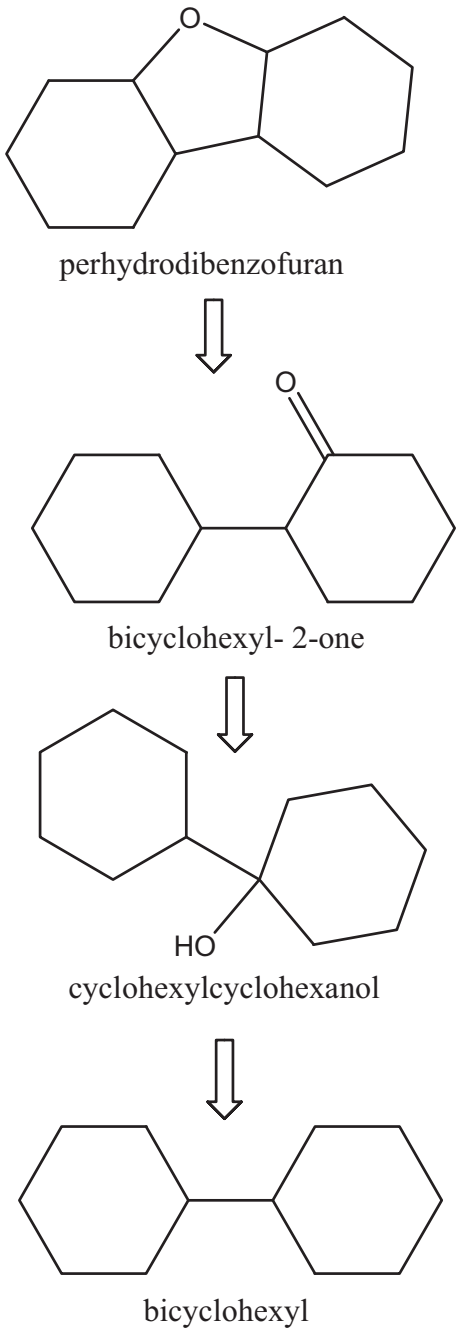

Fig. 7. The products of the ring opening reaction of perhydro-dibenzofuran over ruthenium black catalyst with the proposed order of the reaction steps.

double bonds followed by ring cleavage was previously reported in the hydrogenation of furan over platinum catalyst [38]. On the contrary, it was observed by other group that over a sulfided $NiMo/\gamma\text{-}Al_2O_3$ catalyst, oxygen removal took place prior to the hydrogenation reaction, via a direct reaction [39]. This can be due to the presence of Lewis type active sites on the surface of the sulfided catalyst, as reported in the case of hydroprocessing of nitrogen-containing compounds over Ni-Mo and Ni-W mixed oxide catalysts [40].

Based on the experimentally obtained changes in concentration of the products and intermediates versus time during the course of the reaction, a simplified first order model of the reaction was developed as shown in Fig. 8. For the sake of simplicity, the products

Table 2
Calculated first order rate constants of intermediate reactions of hydrogenation of dibenzofuran over ruthenium black catalyst. Hsis-sum of rate constants of hydrogenolysis reactions.

k_0 (h^{-1})	$k_{0\text{-}4}$ (h^{-1})	$k_{4\text{-}8}$ (h^{-1})	$k_{0\text{-}8}$ (h^{-1})	$k_{0\text{-}12A}$ (h^{-1})	$k_{8\text{-}12B}$ (h^{-1})	$k_{8\text{-}12A}$ (h^{-1})	$k_{12A\text{-}Hsis}$ (h^{-1})	$k_{0\text{-}12B}$ (h^{-1})	$k_{12B\text{-}Hsis}$ (h^{-1})
1.7	0.79	0.61	0.23	0.37	0.96	0.0012	6.2	0.26	0.054

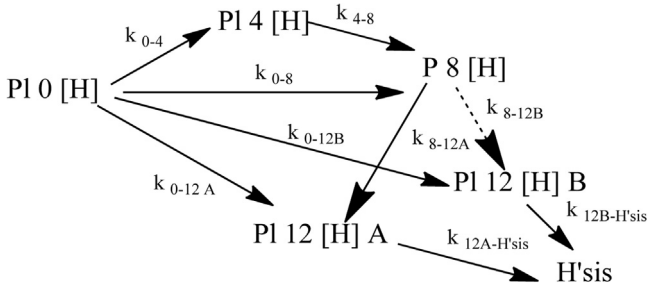

Fig. 8. Simplified first order model of hydrogenation of dibenzofuran followed by hydrogenolysis of C=O bonds of perhydro-dibenzofuran. H'sis-sum of hydrogenolysis products.

of hydrogenolysis of perhydro-dibenzofuran were treated in the model as a sum.

The calculated rate constants for hydrogenation of dibenzofuran are gathered in Table 2. The reaction pathway was described well with the developed model as evidenced in Fig. 9. In order to display more clearly the relevance of the proposed kinetic model, an enlarged part of Fig. 9 containing the products and intermediates which appeared at low concentration is included as Supplementary material, Figure 2s.

It is interesting to note that the rate of hydrogenation of dibenzofuran is almost twice as high as the rate of hydrogenation of carbazole reported in part A of the present work [28]. This is most likely the result of a higher electronegativity of oxygen than nitrogen, which decreases the aromaticity of the dibenzofuran as compared to that of carbazole. Thus, the electrons in dibenzofuran are less uniformly distributed in the Π-orbital, which decreases the overall stability of the aromatic system. Regarding selectivity, dibenzofuran, similarly to carbazole, produces the Pl 8 [H] intermediate in considerable amounts. Furthermore, octahydro-dibenzofuran does not accumulate in the solution as observed in octahydro-carbazole. Thus, the octahydro-dibenzofuran intermediate was converted much faster than its octahydro-carbazole counterpart (3.5 h versus over 6 h). Additionally, the rate constant of octahydro-dibenzofuran formation is significantly lower than the rate constant of its further conversion as evidenced in Table 2.

It is noted that there were several differences observed in the hydrogenation of the oxygen versus nitrogen containing heterocycles under the same reaction conditions. Comparing the products of dibenzofuran hydrogenation to those obtained in the case of carbazole over the same catalyst, the hexahydro-intermediate (Pl 6 [H]) was only formed in the latter. In addition, the hydrogenation of dibenzofuran resulted in the production of two stereoisomers of the fully hydrogenated perhydro-products, as opposed to three stereoisomers that were observed in the hydrogenation of carbazole [28]. Furthermore, unlike carbazole [28] the oxygen containing perhydro-dibenzofuran underwent ring opening reactions under the same reaction conditions. Therefore, based on our results, it can be concluded that the C—O single bonds in the fully saturated cyclic products are more susceptible to rupture than C—N bonds under identical processing conditions.

Despite the fact that the rates of hydrogen loading into dibenzofuran are higher than in the case of hydrogenation of carbazole, the applicability of dibenzofuran in hydrogen storage is strongly inhibited by the possibility of a ring opening reaction during hydrogen loading step and its sluggish kinetics of dehydrogenation as mentioned in the introduction part of this work. Importantly, the presence of hydrogenolysis can affect drastically the fuel recovery process, making the reversible hydrogenation impossible over a ruthenium based catalyst. Nevertheless, it should be taken into account that ruthenium metal has a promoting effect on hydrogenolysis of C—O bond [41]. It is therefore believed that the ring opening of perhydro-dibenzofuran can be eliminated by using catalysts based on other noble metals, which are known to display strong hydrogenation activities and simultaneously hinder bond rupture such as Pt or Ir [42]. Further experimental work would be necessary to verify this point.

The stability of the potential products and intermediates of hydrogenation of dibenzofuran were theoretically studied by DFT methods and the results are shown in Fig. 10 together with the equation used in the calculations. A total of 87 different geometries of intermediates and products were calculated, from which 75

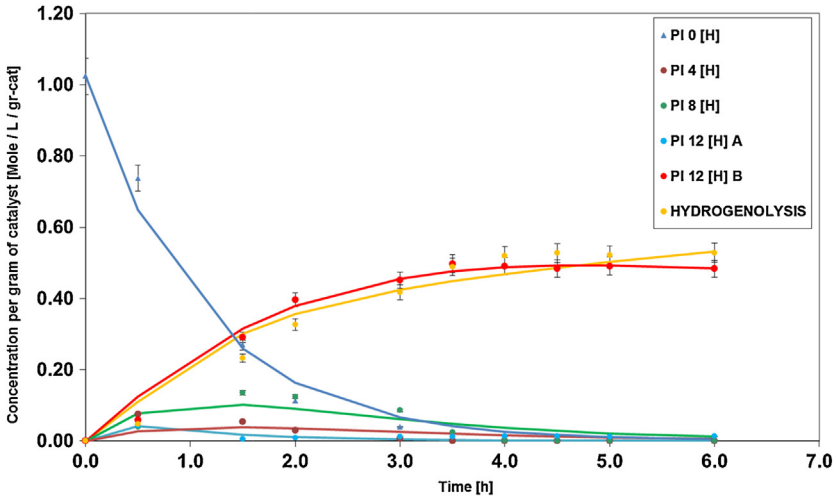

Fig. 9. Product distribution versus time in hydrogenation of dibenzofuran over ruthenium black catalyst.

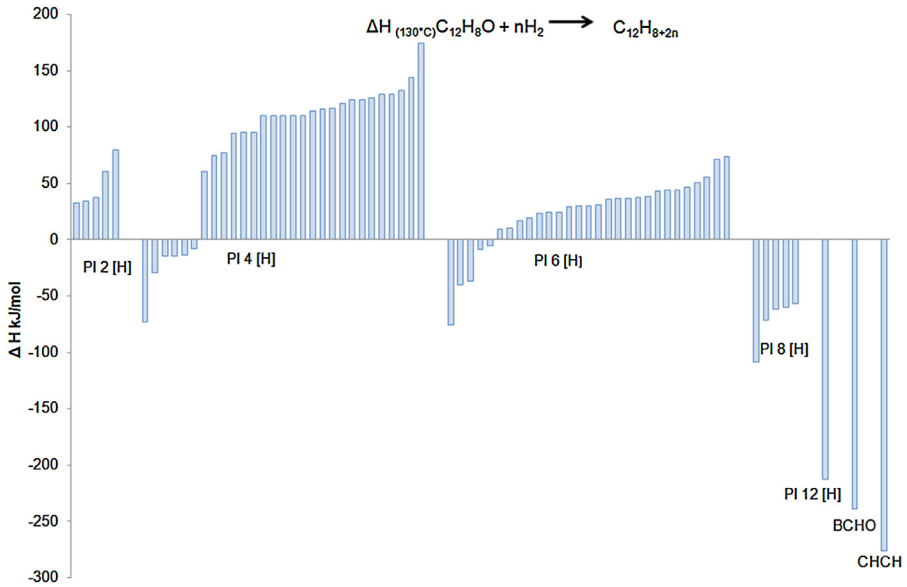

Fig. 10. Results of DFT calculated total enthalpy differences (as indicated in the equation) between the most stable intermediates and products of hydrogenation of dibenzofuran in the gas phase approximation. BCHO—bicyclohexyl 2-one and CHCH—cyclohexylcyclohexanol.

converged to give the respective enthalpy values. From a theoretical point of view, the most stable intermediates and products are those with more negative enthalpy difference. Thus, as it can be seen in Fig. 10, the theoretically expected intermediates in hydrogenation of dibenzofuran are: Pl 4[H], Pl 8 [H], fully saturated Pl 12 [H], CHCH and BCHO which agrees with the experimental observations. However, in our experiments we did not observe the Pl 6 [H] intermediate. Nevertheless, there is a possibility that the Pl 6 [H] could be produced on the surface of the catalyst where it was instantaneously converted to Pl 8 [H] without a desorption step from the surface. Such a subsequent hydrogenation is favourable from the point of view of minimizing the total enthalpy of the system. The discrepancy also exists between the theoretically expected single isomer of Pl 12 [H] and experimentally observed two isomers of Pl 12 [H] A and B. However, it should be noted that this difference can be due to the fact that neither the presence of catalyst nor solvent is taken into account in these DFT calculations. The appearance of different isomers of the fully saturated product is known to be strongly influenced by the type of noble metal present in the catalyst [27].

On the other hand, the theoretical enthalpy difference of Pl 8 [H] (−108.5 kJ/mol) as compared to that of Pl 12 [H] (212.14 kJ/mol) suggests that octahydro-dibenzofuran is not a stable intermediate in the hydrogenation of dibenzofuran, which is in accordance with the experimental data. DFT calculations also showed that the hydrogenolysis of the fully saturated perhydro-dibenzofuran is energetically favourable which also agrees with our experimental observations. The energy difference between Pl 12 [H] and the most stable hydrogenolysis product (CHCH) was calculated to be −63.8 kJ/mol.

3.3.2. Hydrogenation of dibenzothiophene (S)

Similarly to dibenzofuran, dibenzothiophene is a basic compound. Within the middle five-membered thiophene ring fused between two benzenoid rings, a non-hydrogenated S atom employs two electrons to form σ-bonds with the neighboring C atoms and contributes two other electrons to the delocalized Π-system. The last remaining lone pair of electrons is retained by the sulphur atom.

During the hydrogenation of dibenzothiophene, despite the extended reaction times (24 h) and a two-fold increase in the amount of catalyst used (0.3 g vs 0.15 g), not even a trace of any reaction products was observed on GC-MS. The deactivation of a noble metal catalyst in the presence of sulphur containing species is a well-known phenomenon [43]. However an immediate total poisoning of ruthenium catalyst in our work is rather surprising result. Some activity of the catalyst was expected to be present at least at the beginning of the reaction based on the literature reports concerning hydrogenation of dibenzothiophene over noble metal catalyst [44–46]. Apparently, in our case, strong interaction between thiophene and metal surface poisoned most of the small number of active sites on the surface of the Ru black catalyst.

3.3.3. Hydrogenation of fluorene (absence of a heteroatom in the structure)

In order to better understand the impact of carbon replacement by a heteroatom the hydrogenation of homocyclic fluorene was studied. Fluorene is a polycyclic aromatic compound that has a five-membered carbon ring fused between two benzenoid rings (see Fig. 1).

The obtained distribution of products in the hydrogenation of fluorene over ruthenium black catalyst certainly suggested a typical sequential saturation of the aromatic rings. The reaction proceeded with the production of hexahydro-fluorene (Pl 6 [H]) as a primary and major product throughout the reaction. Apart from Pl 6 [H], the production of much lower quantities of two isomers of decahydro-fluorene (Pl 10 [H] A, B) and one isomer of the fully hydrogenated perhydro-fluorene (Pl 12 [H]) was observed. The intermediates and products of fluorene hydrogenation are shown in Fig. 11.

No other products of any side reactions such as hydrogenolysis or isomerisation were observed. It is noteworthy that similar products in the hydrogenation of fluorene over supported Ru, Pd, Pt and Rh were obtained by Sakanishi et al. [23]. However, no Pl 10 [H] intermediates were reported over the studied NiW/Al_2O_3 catalyst [47], which confirms the pronounced influence of the type of the catalytic system on the reaction pathway.

The experimentally obtained changes of concentration in time lead to the development of a reaction model as shown in Fig. 12. The calculated first rate constant based on the experimental consumption of the substrate was only 0.2 h^{-1}. This value is much smaller in comparison to the rate constants obtained in the case of the other similar but heteroaromatic structures studied here such as dibenzofuran (O) −1.7 h^{-1} or carbazole (N) −0.57 h^{-1}. The difference in the rate constants reflects the fact that the presence of a heteroatom

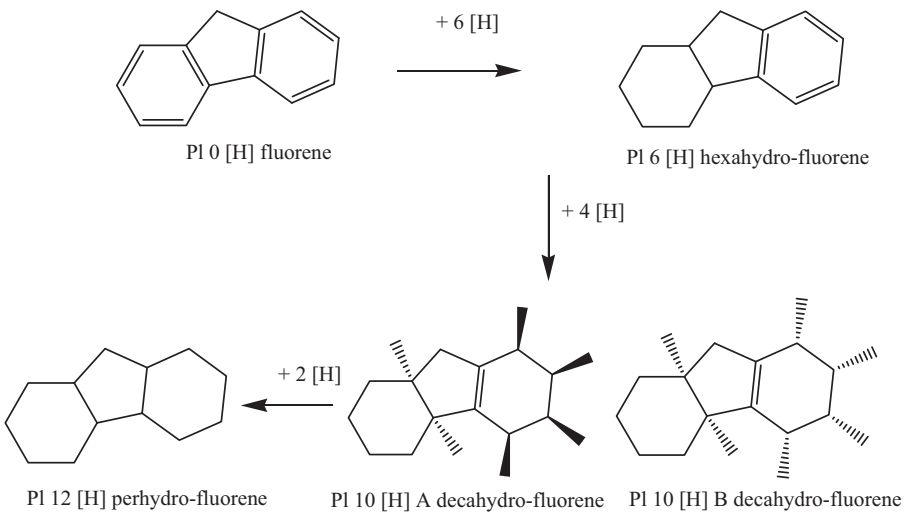

Fig. 11. A simplified scheme containing intermediates and products of catalytic stepwise hydrogenation of fluorene.

in the structure significantly improves the reaction kinetics under the same conditions. As a matter of fact, even after 24 h of extended reaction time the total conversion of fluorene was not reached. This is an extremely slow reaction rate as compared to the hydrogenation of carbazole, where full conversion was reached in a little over 6 h. Overall, the rate of hydrogenation of fluorene was the slowest of all the studied molecules, one of the possible reasons being the higher resonance energy of this molecule. Therefore, a cost effective recyclability of fluorene as a fuel would be a challenging task. Nevertheless, despite the slow rate of hydrogenation, there was only one fully saturated isomer of Pl 12 [H], which is a big advantage from the point of view of the application in LOC based hydrogen storage as discussed before. Moreover, fluorene was previously reported to display a high adsorption strength on the catalyst surface coupled with strong electrostatic interactions of Π-electrons with d electrons of the catalyst surface [18]. Hence, the hydrogenation reaction can take place on multiple C atoms in the benzenoid ring simultaneously on at least one of the benzenoid rings leading to a higher overall selectivity than those obtained with its heterocyclic counterparts. However, a stronger adsorption of fluorene on the catalytic sites unavoidably leads to slower reaction rates.

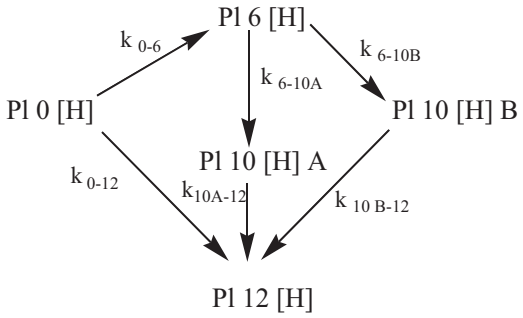

Fig. 12. Simplified first order model for the hydrogenation of fluorene over ruthenium black catalyst. Pl 0[H] is fluorene, Pl 10 [H] A and B are decahydro-fluorene isomers and Pl 12 [H] is perhydro-fluorene.

The experimental product distribution over time was compared with the concentration values calculated using a developed model and the result is shown in Fig. 13 In order to display more clearly the relevance of the proposed kinetic model, an enlarged part of Fig. 13 containing the products and intermediates which appeared at low concentration is included in Supplementary material, Fig. 3s.

The calculated rate constants of all the intermediate reactions expected from the model are gathered in Table 3. As can be observed from these results, the conversion of the starting material towards Pl 6 [H] has the highest rate constant, almost one order of magnitude higher than that of its further conversion to perhydro-fluorene Pl 12 [H]. It is evident that Pl 6 [H] is a primary product of hydrogenation displaying high stability in this reaction. It is formed by the hydrogenation of one of the benzenoid rings adjacent to the five-membered ring. The re-adsorption of the Pl 6 [H] for consecutive saturation is most likely sterically hindered by the fully saturated six-membered ring. The introduction of 6 hydrogen atoms results in significant distortion of the molecule geometry transforming it from planar into boat-like conformation similar to that of cyclohexane. A comparison of the geometries calculated by DFT of the fluorene substrate and of the Pl 6 [H] intermediate is shown in Fig. 14. It is noted that the hexahydro intermediate (Pl 6 [H]) was also observed in the hydrogenation of carbazole, however in much lower concentrations. In addition, the formation of Pl 6[H] in both reactions took place directly from the substrate, via flat adsorption on the catalyst surface.

It is noteworthy that in the absence of a heteroatom in the five-membered ring, the octahydro-intermediate (Pl 8 [H]) is not formed. This intermediate was previously observed in all of the heterocyclic compounds studied, regardless of the type of heteroatom present in the structure. On the contrary, in the hydrogenation of fluorene, the stable intermediate observed was Pl 6 [H], which is evident from the comparison of the rate constants of its formation and its further conversion listed in Table 3. In addition, in the hydrogenation of fluorene, the conversion of Pl 10 [H] A and B intermediates was very sluggish, but the rate constants of sequential hydrogenation of these intermediates to the fully saturated product were higher than the corresponding rate constant of Pl 6 [H].

Table 3
Calculated first order rate constants of intermediate reactions in hydrogenation pathway of fluorene over ruthenium black catalyst.

k_0 (h^{-1})	$k_{0\text{-}6}$ (h^{-1})	$k_{0\text{-}12}$ (h^{-1})	$k_{6\text{-}10A}$ (h^{-1})	$k_{6\text{-}10B}$ (h^{-1})	$k_{10A\text{-}12}$ (h^{-1})	$k_{10B\text{-}12}$ (h^{-1})
0.2	0.19	0.012	0.020	0.028	0.045	0.11

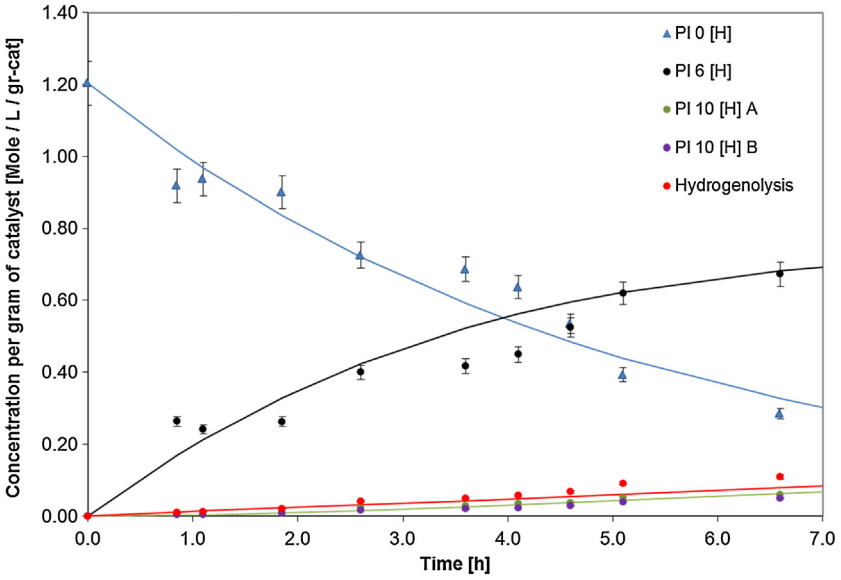

Fig. 13. Product distribution over time in hydrogenation of fluorene. Pl 0 [H] is fluorene, Pl 6 [H] is hexahydro-fluorene, Pl 10 [H] A, B are decahydro-fluorene and Pl 12 [H] is perhydro-fluorene.

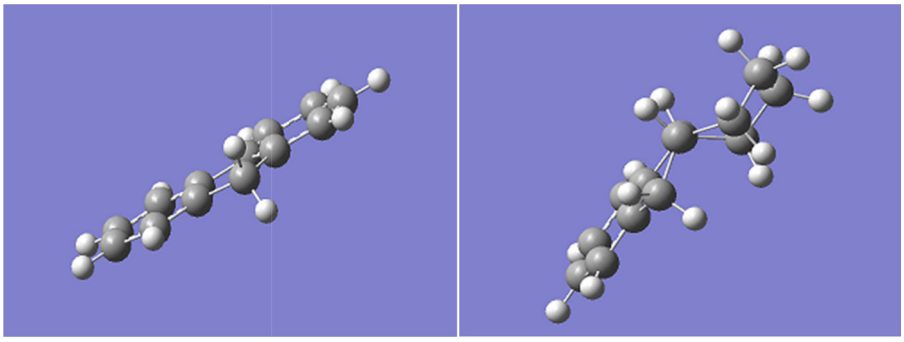

Fig. 14. Geometries calculated by DFT of the fluorene substrate (left) and hexahydro-fluorene Pl 6 [H] intermediate (right) with a boat-like conformation.

Nevertheless, it is interesting to note that the decahydro-intermediates (Pl 10 [H]) were not observed in the hydrogenation of heteroaromatic structures studied in the present work. Moreover, in the hydrogenation of fluorene, there are two isomers of Pl 10 [H] formed by re-adsorption of the Pl 6 [H] intermediate on the catalyst surface. The formation of these stereoisomers can be easily explained. If the addition of 4 hydrogen atoms to Pl 6 [H] takes place on the same side of the molecule, the Pl 10 [H] B cis-isomer is formed. On the other hand, if 4 hydrogen atoms are added to opposite sides of the Pl 6 [H] molecule, the trans-isomer of Pl 10 [H] A product is obtained. Furthermore, it should be noted that upon addition of the remaining 2 hydrogen atoms, there must be further rearrangement/optimisation of the geometry of the Pl 12 [H] product since only one isomer of a fully saturated product has been found in the reaction mixture.

The results of DFT calculations of fluorene are gathered in Fig. 15.

From these results it can be seen that the free enthalpy difference of the Pl 6 [H] intermediate is very low, reaching −108 kJ/mol which is around half of the enthalpy difference of the fully saturated Pl 12 [H] product (−207 kJ/mol). Therefore, this intermediate is thermodynamically very favourable to be produced and additionally it has a theoretical potential to be significantly stable due to the low value of the enthalpy difference. This result agrees well with the experimental observations (see Table 3). In addition, the enthalpy difference of the two isomers of Pl 10 [H] is also low, even lower than that of Pl 6 [H], which also points to these intermediates being fairly stable in the hydrogenation of fluorene. On the other hand, the calculated energies of the system (with no consideration of the activation energy barriers) suggest that it may favour the direct formation of the Pl 12 [H] compound, nevertheless the experimentally observed rate constant of this direct conversion was very low (compare Table 3). This is due to the influence of the catalyst. Additionally, the DFT theoretical considerations suggest the production of Pl 8 [H] intermediate which was not observed experimentally. It might be possible, that Pl 8 [H] was produced on the surface of the catalyst where it was instantly converted to Pl 10 [H] with the theoretical gain in total enthalpy difference of 50 kJ/mol. Similarly, Pl 4 [H] is also theoretically favourable intermediate of this reaction. However, the gain in the total enthalpy of 68 kJ/mol during the conversion of Pl 4 [H] into Pl 6 [H] would make this intermediate less stable in the solution therefore it was not observed experimentally. On the other hand, there is an energy penalty for dihydro-fluorene (Pl 2[H]) and indeed this intermediate was not detected. In addition, the calculated differences in total enthalpy of fluorene and fully saturated perhydro-fluorene (−206.6 kJ/mol) is much smaller than the differences in total enthalpy of carbazole and perhydro-carbazole (−347.6 kJ/mol) reported in our previous work [28]. These results also suggest that the hydrogenation of the latter is a more favourable process, which agrees very well with our experimental results (Fig. 15).

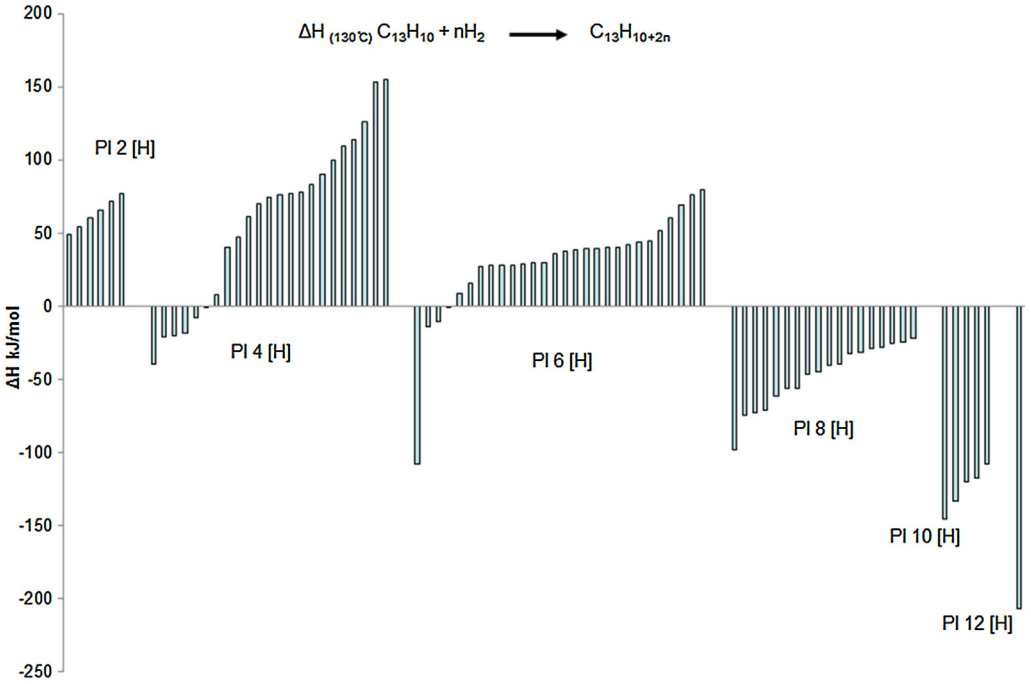

Fig. 15. Results of DFT calculations of total enthalpy differences (as indicated in the equation) between the most stable intermediates and products of hydrogenation of fluorene over Ru black catalyst.

4. Conclusions

With regards to the results presented in the current work, the type and presence of heteroatom plays a crucial role in the optimisation of the carrier structure for hydrogen storage. Importantly, the substitution of C with a heteroatom considerably enhanced the rate of hydrogenation. Higher rates of hydrogenation were also observed in a partially saturated substrate. However, the presence of S in dibenzothiophene was found to immediately poison the Ru black catalyst. On the other hand, despite the high reactivity observed in the hydrogenation of the oxygen containing dibenzofuran, the C—O bonds present in the furan ring were found to be highly susceptible to rupture. It should be noted that the cracking side-reactions have detrimental effect on the recyclability of the LOC and therefore should be avoided.

In general, the selectivity of the hydrogenation reaction was governed by the type and presence of the heteroatom. The amount of isomers of the fully saturated compound was influenced by the type of the heteroatom. In addition, the stable intermediate Pl 8 [H] was only produced during the hydrogenation of heterocyclic compounds. This intermediate however was not always stable for prolonged time. In the hydrogenation of the homocyclic fluorene, the formation of Pl 8 [H] was not observed, but instead Pl 6 [H] was found to be the stable intermediate in this reaction which was explained by the preferable modes of adsorption of substrates and intermediates. Additionally, the DFT calculations of the total enthalpy differences of the theoretically most stable products and intermediates supported the explanation of the experimentally obtained results.

To sum up, based on our extensive studies of various aromatic structures presented here and in part I of the current study [28], it can be concluded that the best candidate for hydrogen storage should contain five membered ring in the structure with a short non-polar side chain. Moreover, in order to increase the rate of reversible hydrogenation and dehydrogenation, the five-membered ring should contain at least one heteroatom. Regarding the type of heteroatom, balancing the rates and selectivity of reversible process, it is clear that the substitution of C with N can offer the most optimum structure design.

Acknowledgements

Mr F. Eblagon, Dr K. Tam from Astra Zeneca, Dr K. M. Kerry Yu and Dr W. Oduro are acknowledged for fruitful discussions and help in data analysis. The authors are indebted to the University of Oxford, EPSRC and to Dr Anibal J. Ramirez-Cuesta from ISIS, UK for financial support of this project.

References

[1] N.Z. Muradova, T. Nejat Vezirog, Int. J. Hydrogen Energy 33 (2008) 6804–6839.
[2] D. Teichmann, W. Arlt, P. Wasserscheid, Int. J. Hydrogen Energy 37 (2012) 18118–18132.
[3] G.A. Olah, Angew. Chem. Int. Ed. 44 (2005) 2636–2639.
[4] D.J. Durbin, C. Malardier-Jugroot, Int. J. Hydrogen Energy 38 (2013) 14595–14617.
[5] J. Du, R. Zhao, G. Jiao, Int. J. Hydrogen Energy 38 (2013) 5789–5795.
[6] F. Alhumaidan, D. Cresswell, A. Garforth, Energ. Fuel 25 (2011) 4217–4234.
[7] F. Alhumaidan, D. Tsakiris, D. Cresswell, A. Garforth, Int. J. Hydrogen Energy 38 (2013) 14010–14026.
[8] M.D. Irfan Hatim, M.A. Umi Fazara, A. Muhammad Syarhabil, F. Riduwan, Procedia Eng. 53 (2013) 71–80.
[9] D. Sebastián, C. Alegre, L. Calvillo, M. Pérez, R. Moliner, M.J. Lázaro, Int. J. Hydrogen Energy 39 (2014) 4109–4115.
[10] K. Morawa Eblagon, K. Tam, K.M.K. Yu, S.-L. Zhao, X.-Q. Gong, H. He, L. Ye, L.-C. Wang, A.J. Ramirez-Cuesta, S.C. Tsang, J. Phys. Chem. C 114 (2010) 9720–9730.
[11] X. Ye, Y. An, G. Xu, J. Alloys Compd. 509 (2011) 152–156.
[12] R.H. Crabtree, Energy Environ. Sci. 1 (2008) 134–138.
[13] P.G. Campbell, L.N. Zakharov, D.J. Grant, D.A. Dixon, S-Y. Liu, J. Am. Chem. Soc. 132 (2010) 3289–3291.
[14] A.U. Pradhan, A. Shukla, J.V. Pande, S. Karmarkar, R.B. Biniwale, Int. J. Hydrogen Energy 36 (2011) 680–688.
[15] A. Shukla, S. Karmakar, R.B. Biniwale, Int. J. Hydrogen Energy 37 (2012) 3719–3726.
[16] E. Clot, O. Eisenstein, R.H. Crabtree, Chem. Commun. 22 (2007) 2231–2233.
[17] Y. Cui, S. Kwok, A. Bucholtz, B. Davis, R.A. Whitney, P.G. Jessop, New J. Chem. 32 (2008) 1027–1037.
[18] F. Sotoodeh, B.J.M. Huber, K.J. Smith, Appl. Catal., A 419–420 (2012) 67–72.
[19] G.P. Pez, A.R. Scott, A.C. Cooper, H. Cheng, US Pat., 7101530, 2006 and prior patents cited.
[20] Z. Wang, J. Belli, C.M. Jensen, Farad. Discuss. 151 (2011) 297–305.
[21] H.Y. Zhao, S.T. Oyama, E.D. Naeem, Catal. Today 149 (2010) 172–184.

[22] F. Sotoodeh, B.J.M. Huber, K.J. Smith, Int. J. Hydrogen Energy 37 (2012) 2715–2722.
[23] K. Sakanishi, M. Ohira, I. Mochida, H. Okazaki, M. Saeda, Bull. Chem. Soc. Jpn. 62 (1989) 3994–4001.
[24] K. Ito, Y. Kogasaka, H. Kurokawa, M. Ohshima, K. Sugiyama, H. Miura, Fuel Proc. Tech. 79 (2002) 77–80.
[25] F. Sotoodeh, K.J. Smith, Ind. Eng. Chem. Res. 49 (2010) 1018–1026.
[26] K. Morawa Eblagon, K. Tam, S.C.E. Tsang, Energy Environ. Sci. 5 (2012) 8621–8630.
[27] K. Morawa Eblagon, K. Tam, K.M.K. Yu, S.C.E. Tsang, J. Phys. Chem. C 116 (2012) 7421–7429.
[28] K. Morawa Eblagon, S.C.E. Tsang, Appl. Catal., B 160–161 (2014) 22–34.
[29] Gaussian 03, revision B.05, Wallingford CT, Gaussian Inc, 2004.
[30] J.B. Foresman, A. Frish, Exploring Chemistry with Electronic Structure Methods, Gaussian Inc., 1998.
[31] M. Nagai, T. Masunaga, Fuel 67 (1987) 771–774.
[32] A. Duan, J. Gao, C. Xu, D. Wang, Z. Zhao, T. Dou, K.H. Chung, Mol. Simul. 33 (2007), 363–359.
[33] P. Crawford, R. Burch, C. Hardacre, K.T. Hindle, P. Hu, D.W. Rooney, J. Chem. Phys. 128 (2008) 105104-1–105104-6.
[34] G.P. Pez, A.R. Scott, A.C. Cooper, H. Cheng, F.C. Wilhelm, A.H. Abdourazak, US Pat., 7351395, 2008 and prior patents cited.
[35] P. Crawford, R. Burch, C. Hardacre, K.T. Hindle, P. Hu, B. Kalirai, D.W. Rooney, J. Phys. Chem. C 111 (2007) 6434–6439.
[36] R.R. Gupta, T.M. Krygowski, M.K. Cyranski, Aromaticity in Heterocyclic Compounds, Springer-Verlag, Berlin, 2009.
[37] L.D. Rollman, J. Catal. 46 (1977) 243–252.
[38] H.A. Smith, J.F. Fuzek, J. Am. Chem. Soc. (1949) 415–419.
[39] S. Krishnamurthy, S. Panvelker, Y.T. Shah, AlchE J. 27 (1981) 994–1001.
[40] C. Moreu, C. Aubert, R. Durand, N. Zmimita, P. Geneste, Catal. Today 4 (1988) 117–131.
[41] J. Shabtai, G.J.C. Yeh, C. Russell, A.G. Oblad, Eng. Chem. Res. 28 (1989) 139–146.
[42] M. Jacquin, D.J. Jones, J. Rozière, S. Albertazzi, A. Vaccari, M. Lenarda, L. Storaro, R. Ganzerla, Appl. Catal., A 131 (2003) 131–141.
[43] S. Albertazzi, E. Rodríguez-Castellón, M. Livi, A. Jiménez-López, A. Vaccari, J. Catal. 228 (2004) 218–224.
[44] W. Qian, Y. Yoda, Y. Hirai, A. Ishihara, T. Kabe, Appl. Catal., A 184 (1999) 81–88.
[45] T. Kabe, W. Qian, Y. Hirai, L. Li, A. Ishihara, J. Catal. 190 (2000) 191–198.
[46] R.M. Navarro, B. Pawelec, J.M. Trejo, R. Mariscal, J.L.G. Fierro, J. Catal. 189 (2000) 184–194.
[47] A.T. Lapinas, M.T. Klein, B.C. Gates, Ind. Eng. Chem. Res. 30 (1991) 42–50.